

Integrin function and misfunction

- **Integrins** transduce information from the ECM (extracellular matrix) to the cell as well as reveal the status of the cell to the outside, allowing rapid and flexible responses to changes in the environment. They are cell surface receptors that interact with the ECM and mediate various intracellular signals. They play key roles in tissue integrity, cell trafficking, and control diverse cell functions.

The two main functions of integrins are:

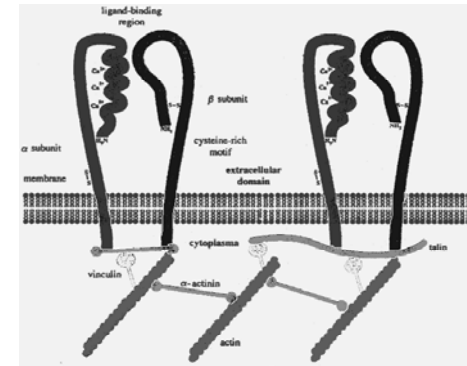
1) **Signal transduction** from the ECM to the cell.

The signals involve: cell growth, cell migration, cell division, cell survival, cellular differentiation, apoptosis (programmed cell death)

2) **Attachment of the cell** to other cells and to the **ECM**.

- Disturbance of integrin function is connected to a large variety of pathological processes such as thrombosis, cancer, osteoporosis and inflammation, which makes integrins attractive targets for pharmacological research.

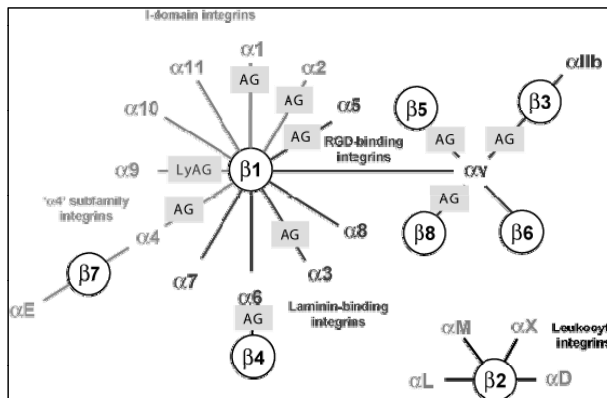
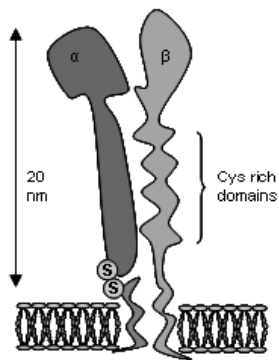
INTEGRINS



- Integrins are one of the major families of cell adhesion receptors.
- They are transmembrane bidirectional receptors, containing large extracellular domains and short cytoplasmic domains, which connect cells to the scaffolding proteins of the extracellular matrix (ECM).
- On the extracellular face, integrins engage either ECM-macromolecules or counter-receptors on adjacent cell surfaces.
- On the cytoplasmic face of the plasma membrane, integrin occupancy coordinates the assembly of cytoskeletal polymers and signaling complexes.

INTEGRINS

- All integrins are non-covalently linked, heterodimeric glycoproteins containing an α (alpha) and β (beta) subunit.
- 18 alpha and 8 beta subunits are known, forming 24 different $\alpha\beta$ heterodimers.



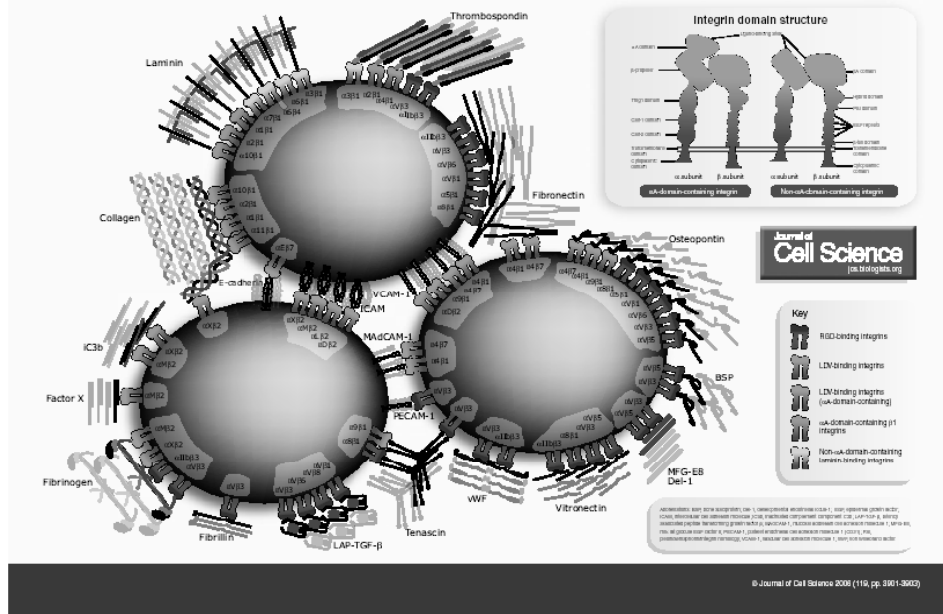
Integrin subfamilies: the RGD-binding integrins (blue), the laminin-binding integrins (red), the leukocyte integrins (black), the I-domain-containing integrins (green), and the $\alpha 4$ sub-family integrins (pink). AG, role of this integrin in angiogenesis.

RGD-Binding Integrins

- Most integrin receptors are able to bind a wide variety of ligands.
- Moreover, many extracellular matrix and cell surface adhesion proteins bind to multiple integrin receptors.
- All five α_V integrins, two β_1 integrins (α_5, α_8) and $\alpha_{IIb}\beta_3$ share the ability to recognise ligands containing an **RGD** tripeptide active site.
- The RGD-binding integrins are among the most promiscuous in the family, with β_3 integrins in particular binding to a large number of extracellular matrix and soluble vascular ligands.

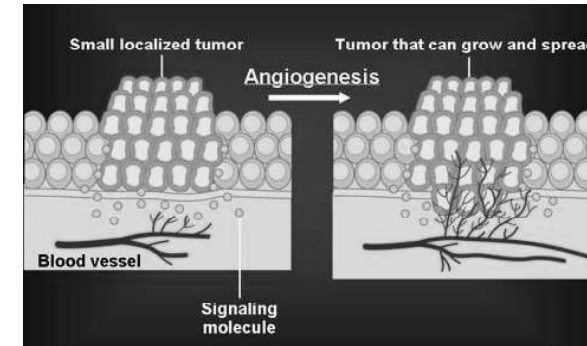
Integrin Ligands at a Glance

Jonathan D. Humphries, Adam Byron and Martin J. Humphries



RGD-binding Integrins: a central role in mediating ANGIOGENESIS

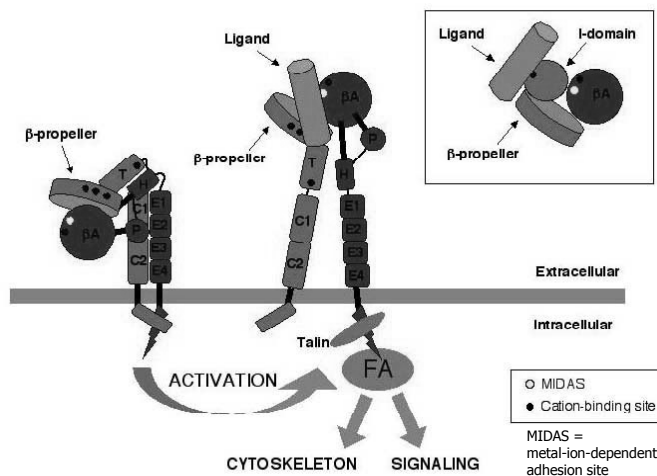
- Of the 24 different heterodimers known, the RGD-binding integrins $\alpha_V\beta_3$, $\alpha_V\beta_5$, $\alpha_5\beta_1$ are key-factors of angiogenesis (the formation and maturation of new blood vessels), an important process in tumor progression and metastasis.



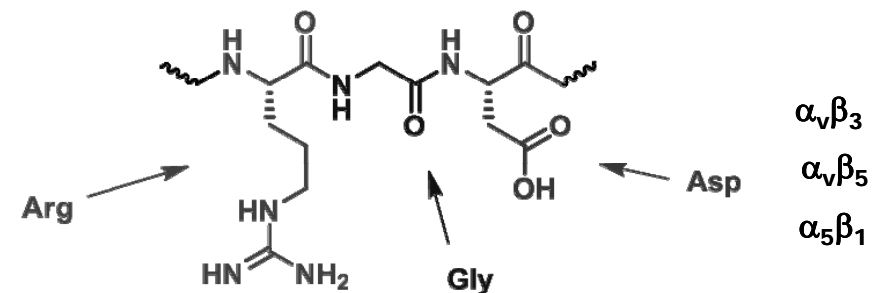
Angiogenesis (new blood vessel formation) plays a pivotal role in tumor growth and metastatic spreading

RGD-Binding Integrins

- Crystal structures of $\alpha_V\beta_3$ and $\alpha_{IIb}\beta_3$ complexed with RGD ligands have revealed an identical atomic basis for this interaction.
- RGD binds at an interface between the α and β subunits, the R (arginine) residue fitting into a cleft in a β -propeller module in the α subunit, and the D (aspartate) coordinating a cation bound in the β subunit.

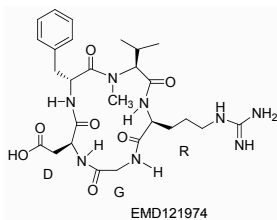


RGD INTEGRIN RECOGNITION SEQUENCE



- Particular integrins are able to selectively bind different spatial presentations of a single binding motif (RGD) in multiple ECM proteins. **Specificity** is determined by: (a) flanking residues, (b) 3D presentation, (c) features of the binding pocket.
- Synthetic RGD-ligands can bind to integrins and inhibit endogenous ligand binding with an RGD-recognition specificity.
- Selective RGD-ligands of alphaV/beta3 and/or alphaV/beta5 integrins significantly inhibit vessel development and tumor growth.**

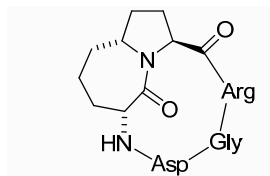
RGD-ligands for integrins



Cilengitide

The potent $\alpha_v\beta_3$ ligand, cyclic peptide Cilengitide (H. Kessler et al., *J. Med. Chem.* **1999**, *42*, 3033) cyclo-[Arg-Gly-Asp-D-Phe-N(Me)-Val], is currently in phase III clinical trials for patients with glioblastoma multiforme

Inhibition of biotinylated vitronectin binding to $\alpha_v\beta_3$ receptor
 $\alpha_v\beta_3$ IC₅₀ 0.58 nM

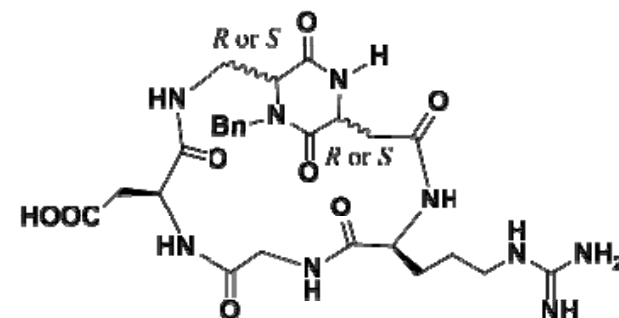


ST 1646

Cyclic RGD pentapeptide mimics cyclo(Arg-Gly-Asp-lactam)
 (C. Scolastico et al., *Org. Lett.* **2001**, *3*, 1001)
 (C. Scolastico et al., *ChemMedChem* **2009**, *4*, 615)

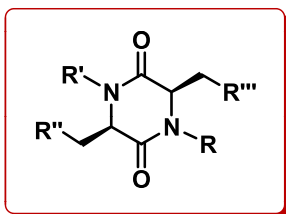
Inhibition of biotinylated vitronectin binding to integrin receptors
 $\alpha_v\beta_3$ IC₅₀ 1.0 ± 0.5 nM
 $\alpha_v\beta_5$ IC₅₀ 1.4 ± 0.8 nM

Diketopiperazine RGD-ligands for integrins



- Efficient synthesis (in solution) of constrained peptides containing the **Arg-Gly-Asp** (RGD) motif
- Conformational analysis by NMR and molecular modelling
- Binding affinity studies to the $\alpha_v\beta_3$ and $\alpha_v\beta_5$ integrin receptors

Diketopiperazines (DKPs)



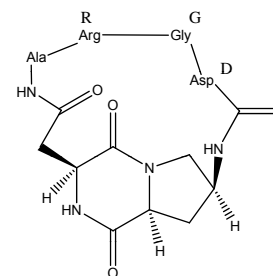
1. smallest cyclic peptides
2. simple heterocyclic scaffolds, easy to synthesise
3. functional diversity
4. conformational rigidity
5. H-bonds
6. resistance to proteolysis



- privileged structures for drug discovery
- useful scaffolds for peptidomimetics
- organic catalysts

Fischer, P. *J. Peptide Sci.* **2003**, *9*, 9.

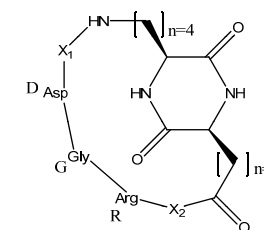
Diketopiperazine RGD-ligands for integrins



Cis-diketopiperazine

(Robinson et al., *Helv. Chim. Acta* **1996**, *79*, 1825)

Inhibition of fibrinogen binding to $\alpha_v\beta_3$ receptor
 $\alpha_v\beta_3$ IC₅₀ 0.1 μ M



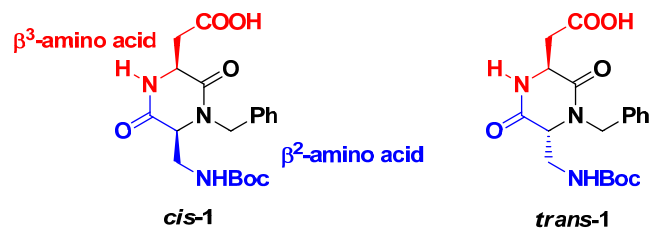
Cis-diketopiperazines

(Albericio et al., *Tetrahedron Lett.* **2001**, *42*, 7387)

Inhibition of echistatin* binding to $\alpha_v\beta_3$ receptor
 $\alpha_v\beta_3$ IC₅₀ 4-8 ± 2 μ M

*Echistatin, an RGD-containing snake venom peptide (49 aa) with high affinity for β_3 integrins

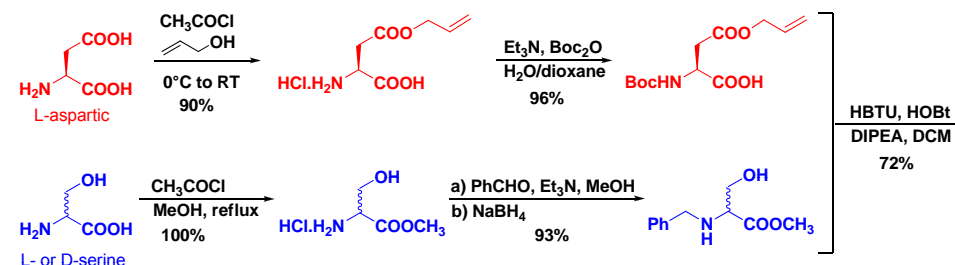
Diketopiperazine scaffolds



- The two reactive functionalities can be locked in a *cis*- or *trans*-relationship as a consequence of the absolute configurations of the two α -amino acids.
- DKP scaffold 1, while being derived from α -amino acids can be seen as a constrained dipeptide formed by two β -amino acids, and in particular a β^2 and a β^3 -amino acids (following Seebach's nomenclature).

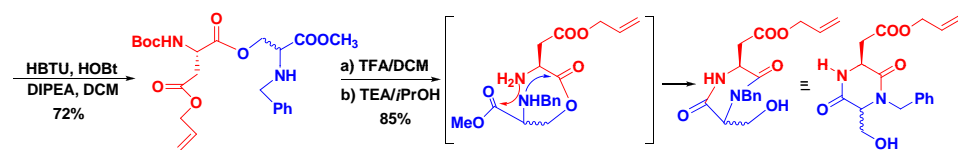
Ana Sofia M. Ressurreição, Andrea Bordessa, Monica Civera, Laura Belvisi, Cesare Gennari, Umberto Piarulli *J. Org. Chem.* **2008**, 73 (2), 652-660.

Synthesis of *cis* and *trans*-DKP-1



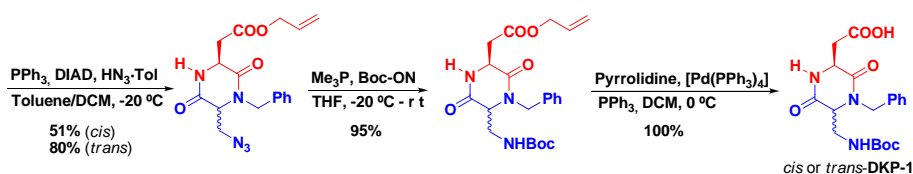
Ana Sofia M. Ressurreição, Andrea Bordessa, Monica Civera, Laura Belvisi, Cesare Gennari, Umberto Piarulli *J. Org. Chem.* **2008**, 73 (2), 652-660.

Synthesis of *cis* and *trans*-DKP-1



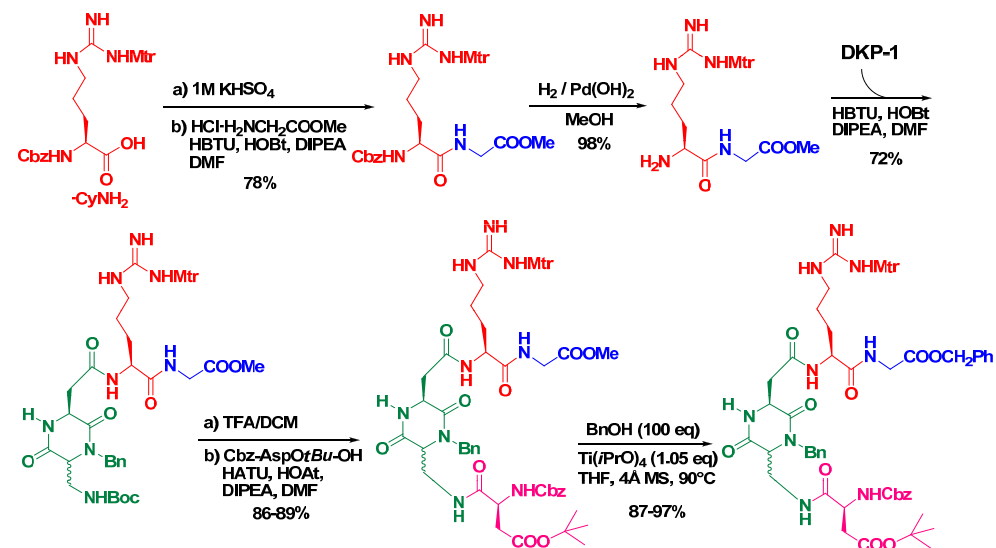
HMBC (Heteronuclear Multiple Bond Correlation) spectrum

M. Marchini, M. Mingozzi, R. Colombo, C. Gennari, M. Durini, U. Piarulli, *Tetrahedron*, submitted.



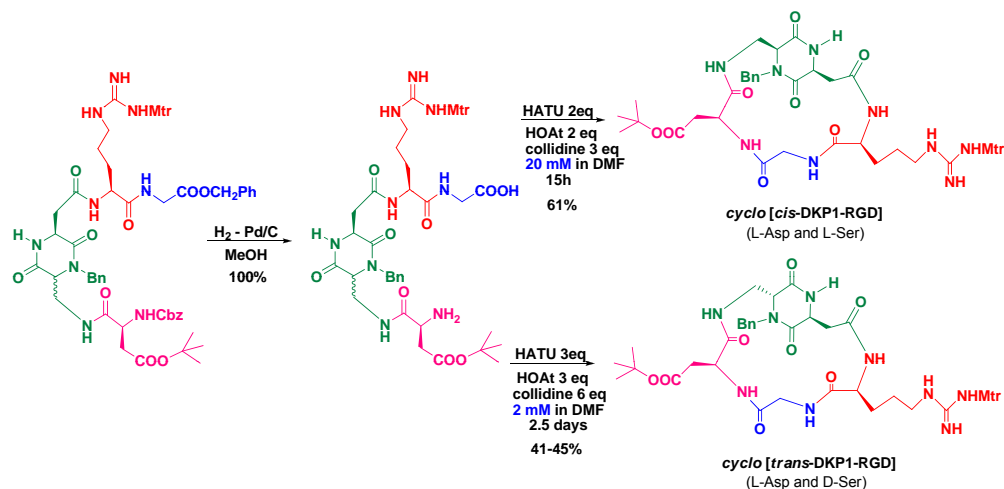
cis or *trans*-DKP-1

Synthesis of cyclic-RGD peptidomimetics

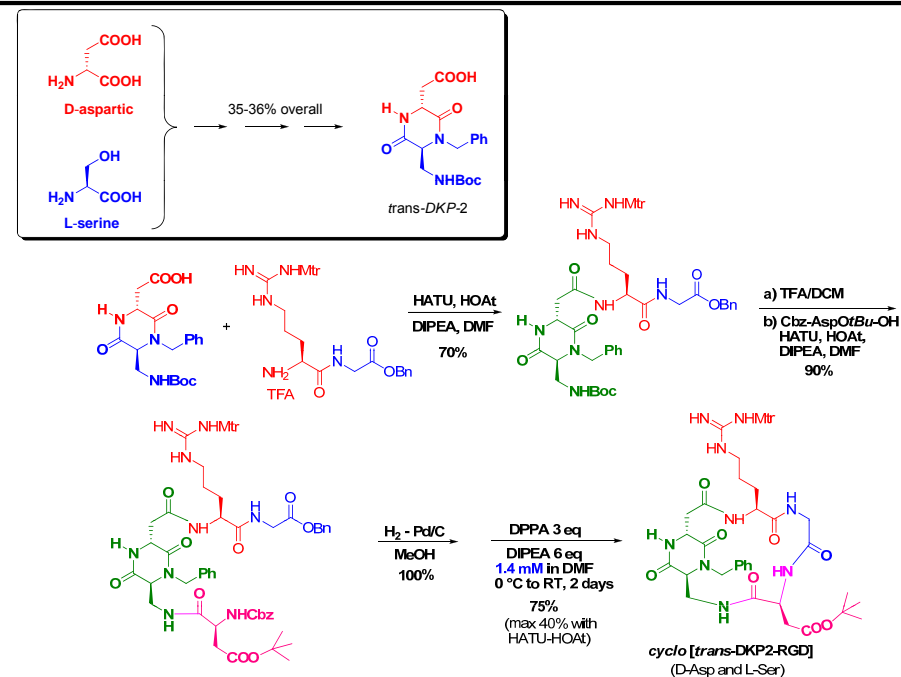


Mtr = 4-Methoxy-2,3,6-trimethylbenzenesulfonyl

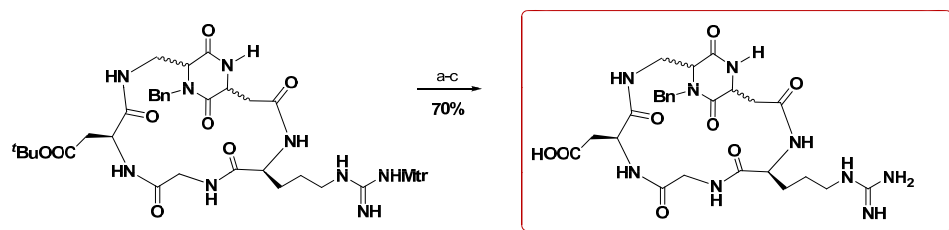
Synthesis of cyclic-RGD peptidomimetics



Synthesis of cyclic-RGD peptidomimetics



Biological Results



- a) "Cleavage cocktail": TFA (80%), triethylsilane (2.5%), ethanedithiol (5%), phenol (5%), thioanisole (5%), H₂O (2.5%)
 b) HPLC purification, c) Lyophilization

Inhibition of biotinylated vitronectin binding to $\alpha_v\beta_3$ and $\alpha_v\beta_5$ receptors

| Compound | $\alpha_v\beta_3$ IC ₅₀ [nM] | $\alpha_v\beta_5$ IC ₅₀ [nM] |
|------------------------|--|--|
| Cyclo [cis-DKP1-RGD] | 3898 ± 418 | > 10 ⁴ |
| Cyclo [trans-DKP1-RGD] | 3.2 ± 2.7 | 114 ± 99 |
| Cyclo [trans-DKP2-RGD] | 4.5 ± 1.1 | 149 ± 25 |
| c(RGDfV) | 3.2 ± 1.3 | 7.5 ± 4.8 |
| ST1646 | 1.0 ± 0.5 | 1.4 ± 0.8 |

A. S. M. da Ressurreição, A. Vidu, M. Civera, L. Belvisi, D. Potenza, L. Manzoni, S. Ongeri, C. Gennari, U. Piarulli
Chemistry - A European Journal 2009, 15, 12184-12188.

Biological Results

Adhesion assay experiments performed on a panel of human epithelial cancer cell lines
 (Multiforme Glioblastoma, Bladder and Breast Adenocarcinomas)

| Compound | ECV304 (Bladder adenocarcinoma) IC ₅₀ μ M | | T98G (Multiforme Glioblastoma) IC ₅₀ μ M | | MDA-MB-231 (Breast adenocarcinoma) IC ₅₀ μ M | |
|------------------------|--|-------------|---|-------------|---|-----------|
| | VN | FN | VN | FN | VN | FN |
| Cyclo [cis-DKP1-RGD] | >> 200 | >> 200 | >> 200 | >> 200 | >> 200 | >> 200 |
| Cyclo [trans-DKP1-RGD] | 49.5 ± 3.0 | 15.0 ± 3.9 | 8.4 ± 0.8 | 1.9 ± 0.5 | 6.8 ± 2.9 | 3.0 ± 0.9 |
| Cyclo [trans-DKP2-RGD] | 13.8 ± 0.2 | 2.2 ± 0.4 | 3.0 ± 0.7 | 0.8 ± 0.1 | 1.6 ± 0.0 | 0.7 ± 0.1 |
| c(RGDfV) | 0.22 ± 0.00 | 0.36 ± 0.09 | 0.14 ± 0.03 | 0.12 ± 0.03 | 11.3 ± 0.1 | 3.4 ± 0.4 |

| Cell line | MFI | | | Expression $\alpha_5\beta_1 / \alpha_v\beta_3$ |
|------------|----------------------------|----------------------------|----------------------------|---|
| | $\alpha_v\beta_5$ integrin | $\alpha_v\beta_3$ integrin | $\alpha_5\beta_1$ integrin | |
| ECV304 | 1977 | 3322 | 3867 | 1.16 |
| T98G | 1663 | 4741 | 13041 | 2.75 |
| MDA-MB-231 | 795 | 592 | 4208 | 7.11 |

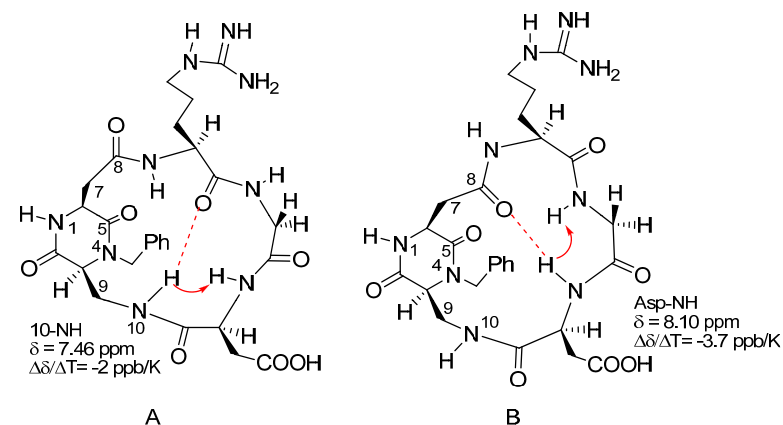
MFI: Mean Fluorescence Intensity

Elena Araldi, CISI, Milano

**NMR and computational studies
of Cyclo [*cis*-DKP1-RGD],
Cyclo [*trans*-DKP1-RGD] and Cyclo [*trans*-DKP2-RGD]**

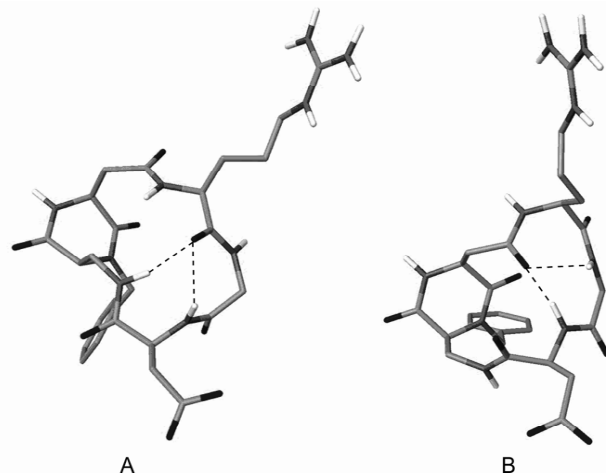
- Fully characterized by ¹H- and ¹³C-NMR spectroscopy (9:1 H₂O-D₂O)
- Intramolecular hydrogen bonds were detected by measuring the chemical shift of the N-H protons and their temperature coefficients ($\Delta\delta/\Delta T$) in dilute solutions
- NOESY spectra were recorded to investigate both sequential and long-range NOE's that provide evidences of preferred conformations
- Three-dimensional structures satisfying long-range NOE contacts were generated by restrained mixed-mode Metropolis Monte Carlo/Stochastic Dynamics (MC/SD) simulations, using the implicit water GB/SA solvation model

NMR Studies of Cyclo [*cis*-DKP1-RGD]



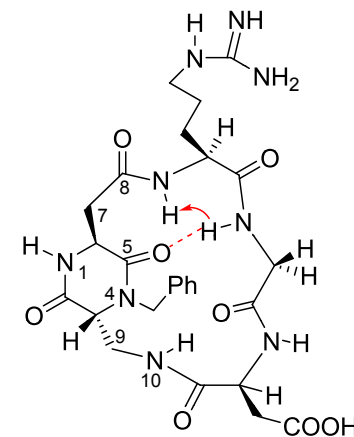
Preferred intramolecular hydrogen-bonded patterns proposed for [*cis*-DKP1-RGD] on the basis of spectroscopic data. (A) β -turn at Gly-Asp. (B) β -turn at Arg-Gly. The arrows indicate significant, mutually exclusive, NOE contacts.

Computational Studies of Cyclo [*cis*-DKP1-RGD]



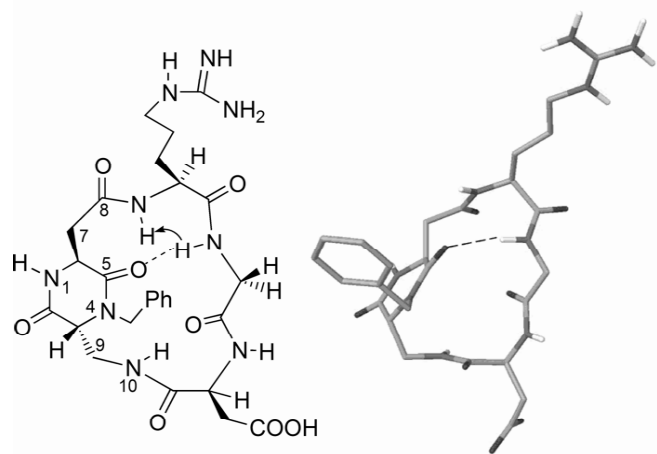
Structures of [*cis*-DKP1-RGD] as obtained by restrained MC/SD simulations (10 ns) based on NOESY spectra NH10/Asp-NH or Asp-NH/Gly-NH distance information. (A) β II'-turn at Gly-Asp and γ -turn at Gly [average C β (Arg)-C β (Asp) distance = 7.4 Å]. (B) β II'-turn at Arg-Gly and γ -turn at Arg [average C β (Arg)-C β (Asp) distance = 6.5 Å]. In both cases: **non-extended** arrangement of the RGD sequence.

NMR Studies of Cyclo [*trans*-DKP1-RGD]



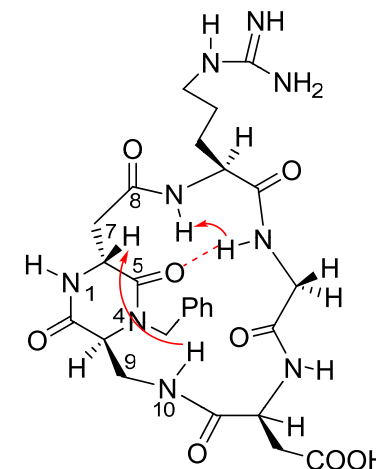
Preferred intramolecular hydrogen-bonded pattern proposed for [*trans*-DKP1-RGD] on the basis of spectroscopic data. The arrow indicates a significant NOE contact.

Computational Studies of Cyclo [*trans*-DKP1-RGD]



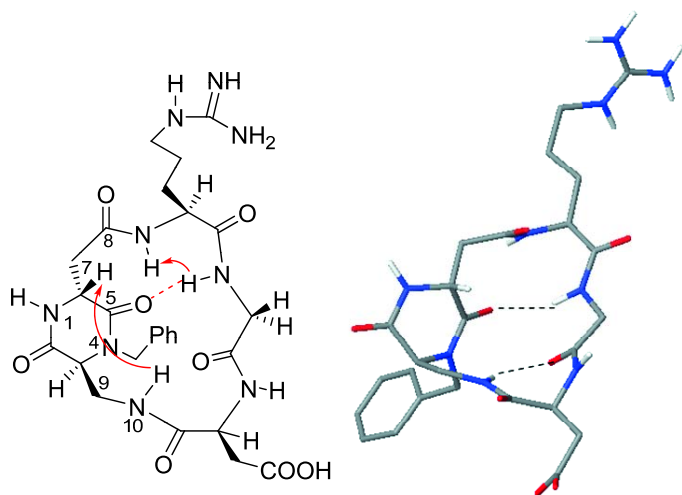
Structure of [**trans-DKP1-RGD**] as obtained by restrained MC/SD simulation (10 ns) based on NOESY spectra Gly-NH/Arg-NH distance information. Pseudo β -turn at DKP-Arg, distorted inverse γ -turn at Asp [average C β (Arg)-C β (Asp) distance = 9.3 Å]: **extended** arrangement of the RGD sequence.

NMR Studies of Cyclo [*trans*-DKP2-RGD]



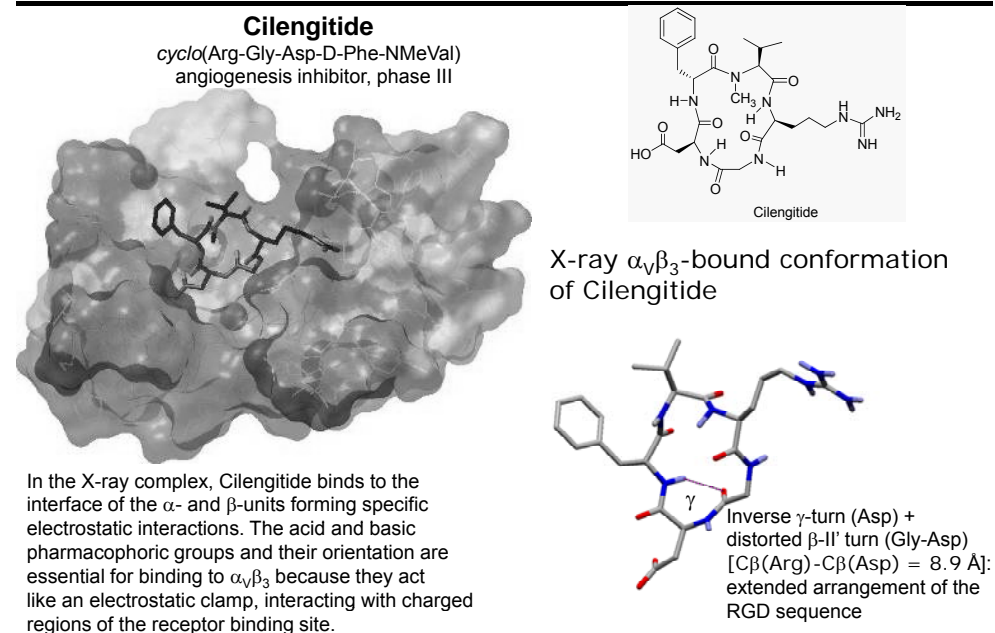
Preferred intramolecular hydrogen-bonded pattern proposed for [**trans-DKP2-RGD**] on the basis of spectroscopic data. The arrows indicate significant NOE contacts.

Computational Studies of Cyclo [*trans*-DKP2-RGD]



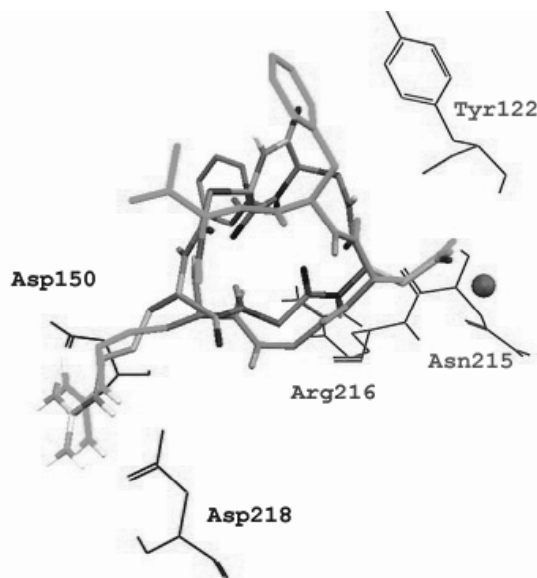
Structure of [**trans-DKP2-RGD**] as obtained by restrained MC/SD simulation (10 ns) based on NOESY spectra distance information. Pseudo β -turn at DKP-Arg, inverse γ -turn at Asp [average C β (Arg)-C β (Asp) distance = 8.8 Å]: **extended** arrangement of the RGD sequence.

X-ray structure $\alpha_v\beta_3$ integrin-Cilengitide



Kessler, H. et al. *J. Med. Chem.* **1999**, *42*, 3033.
 Arnout, M. et al. *Science*, **2002**, *296*, 151.

Docking Studies - [*trans*-DKP1-RGD]

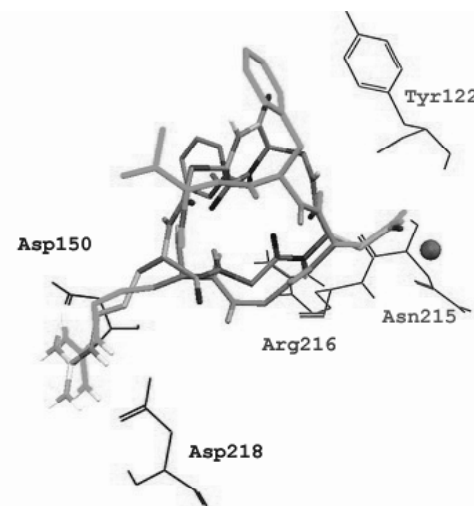


Top-ranking binding mode of [*trans*-DKP1-RGD] ligand into the crystal structure of the extracellular domain of $\alpha_v\beta_3$ integrin overlaid on the bound conformation of Cilengitide (green).

Red: residues of α subunit
Blue: residues of β subunit
Green: Cilengitide

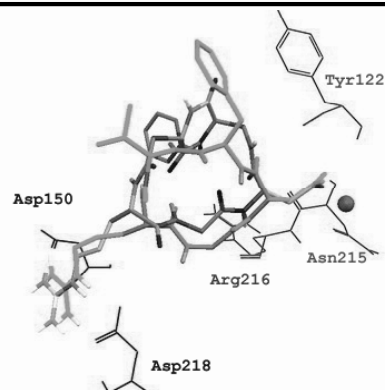
The Mn^{2+} ion at MIDAS (metal-ion-dependent adhesion site) is shown as a magenta CPK sphere

Docking Studies - [*trans*-DKP1-RGD]



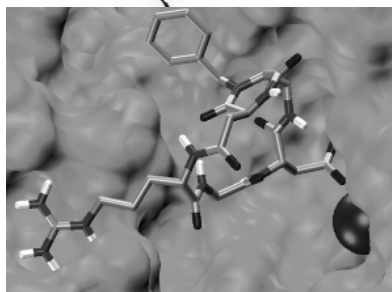
Docking calculations starting from the extended geometry of [*trans*-DKP1-RGD] conserved all the important interactions of the X-ray complex. The positively charged Arg guanidinium group of the ligand interacts with the negatively charged side chains of Asp218 and Asp150 in the α unit, one carboxylate oxygen of the ligand Asp side chain is coordinated to the metal cation in the metal-ion-dependent-adhesion-site (MIDAS) region of the β unit, while the second carboxylate oxygen forms hydrogen bonds with the backbone amides of Asn215 and Tyr122 in the β unit. Further stabilizing interaction involves the formation of a hydrogen bond between the ligand backbone NH of the Asp residue and the backbone carbonyl group of Arg216 in the β unit.

Docking Studies - [*trans*-DKP1-RGD]



The micromolar affinity of [*cis*-DKP1-RGD] for $\alpha_v\beta_3$ can be explained in terms of its low pre-organization for binding. In fact, [*cis*-DKP1-RGD] in solution mainly features non-extended RGD conformations which, according to the docking results, are not able to properly fit into the $\alpha_v\beta_3$ receptor: optimal interactions are conserved only with the α -subunit of the $\alpha_v\beta_3$ receptor.

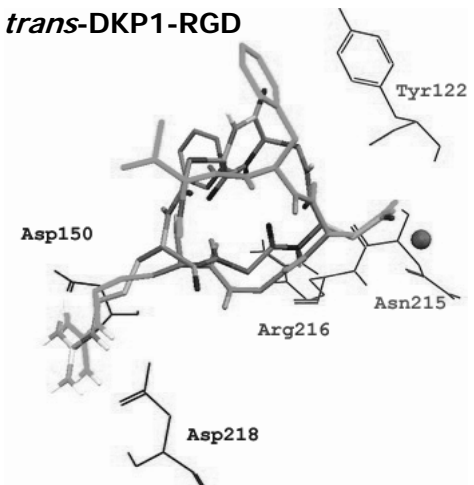
On the contrary, the low nanomolar affinity of [*trans*-DKP1-RGD] for $\alpha_v\beta_3$ can be attributed to its high structural pre-organization. The *trans*-DKP1 scaffold induces a preferred conformation with Arg in the *i*+1 position of a pseudo β -turn which determines an extended RGD disposition similar to the RGD bound conformation of Cilengitide.



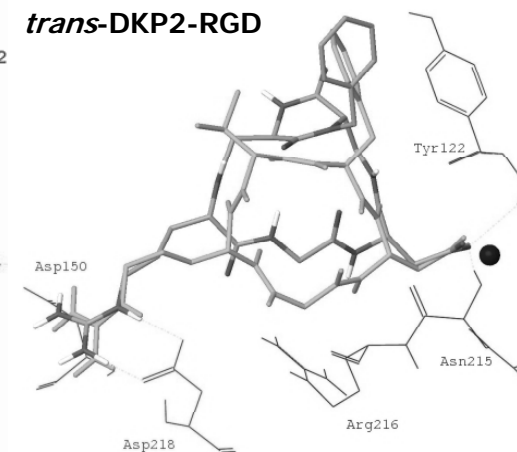
Docking Studies - [*trans*-DKP1-RGD] and [*trans*-DKP2-RGD]

Top-ranking binding mode of ligands into the crystal structure of the extracellular domain of $\alpha_v\beta_3$ integrin overlaid on the bound conformation of Cilengitide (green).

trans-DKP1-RGD

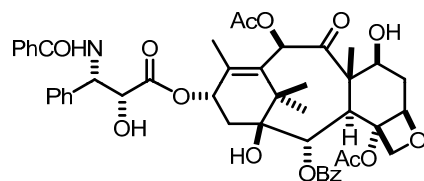


trans-DKP2-RGD



Red: residues of α subunit Blue: residues of β subunit Green: Cilengitide
The Mn^{2+} ion at MIDAS (metal-ion-dependent adhesion site) is shown as a magenta CPK sphere

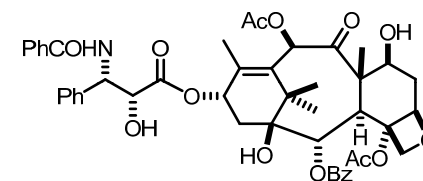
Taxol



Taxol® (Paclitaxel)

- Isolated from the bark of the pacific yew *Taxus Brevifolia*
- The complex diterpene Taxol is probably the most well known cancer chemotherapeutic agent of natural origin and it is approved for the treatment of metastatic breast cancer, metastatic cancer of the ovary, Kaposi's sarcoma and non-small cell lung cancer
- Taxol inhibits cancer cell growth through the stabilization of cellular microtubules and interference with microtubule dynamics
- The most severe limitations to the clinical application of Taxol® are:
 - a) Taxol is not selective for cancerous cells. This causes severe toxic side-effects
 - b) the emergence of the "Multiple Drug Resistance" (MDR)

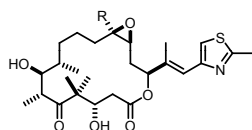
Limitations of Taxol: MDR



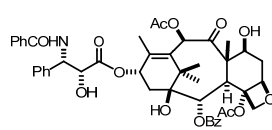
Taxol® (Paclitaxel)

- MDR consists in the emergence of tumor phenotypes resistant to taxanes
- This phenomenon (MDR) results from two mechanisms:
 - a) over-expression of the P-glycoprotein (PgP), an ATP dependant efflux pump that lowers the intracellular concentration of cytotoxic products, on the surface of neoplastic cells
 - b) over-expression of tubulin isotypes (e.g. β III isotype) that are less susceptible to induced polymerization and stabilization
- The discovery of alternative natural products endowed with a Taxol-like mode of action, but active against Taxol®-resistant tumor cell lines, is a relatively recent achievement

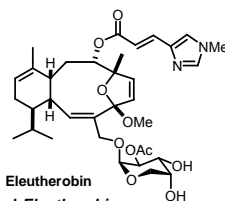
Natural Products with Tubulin polymerization and microtubule stabilization properties



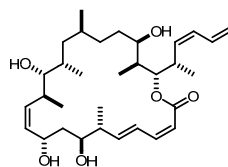
Epothilone A : R = H
Epothilone B : R = Me
Myxobacterium
Sorangium cellulosum



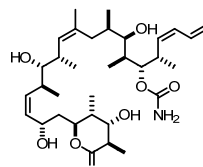
Taxol® (Paclitaxel)
Taxus brevifolia



Eleutherobin
Coral *Eleutherobia*



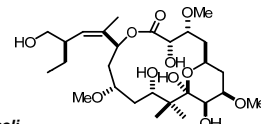
Dictyostatin
Sponge *Lithistidia*



Discodermolide
Sponge *Discodermia dissoluta*

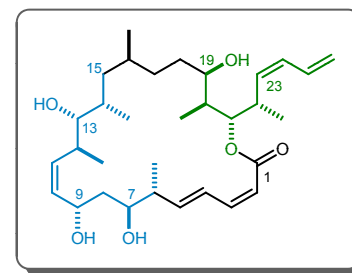


Lauimalide Sponge *Hyattella*

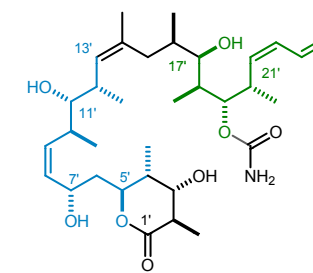


Sponge *Mycale hentscheli* Peloruside A

Dictyostatin



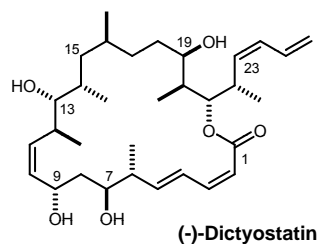
(-)-Dictyostatin



(+)-Discodermolide

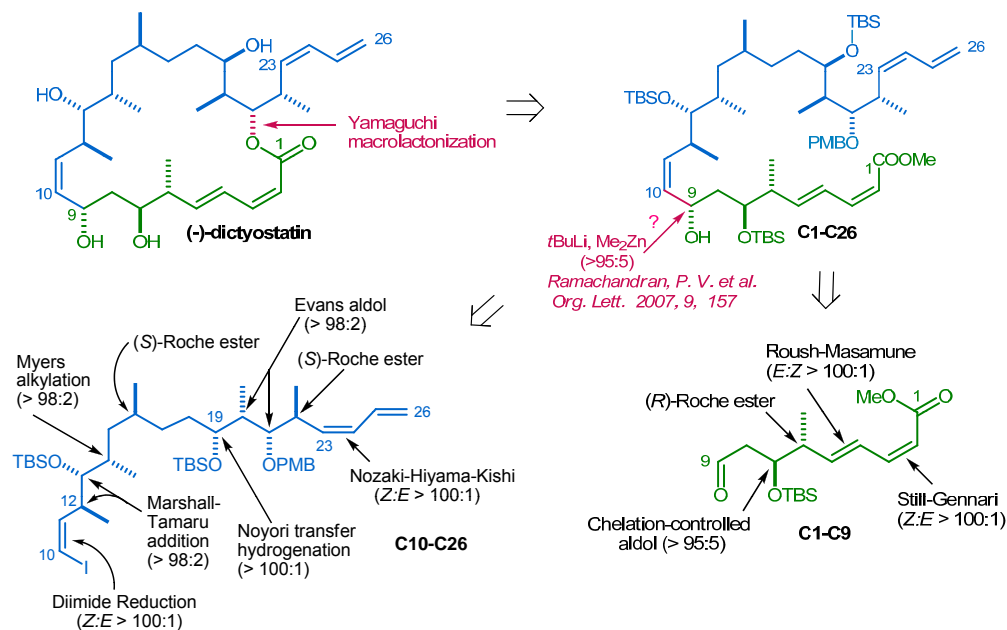
- Dictyostatin was isolated by Pettit *et al.* in 1994 (only 1.35 mg from over 400 kg sponge). The revised structure and newly assigned stereochemistry of Dictyostatin (Paterson, 2004) demonstrates its analogy to Discodermolide
- Dictyostatin demonstrates an exceptional cytotoxic activity (ED50 0.38 nM, P338 leukemia cells), even superior to the already very potent Discodermolide
- Dictyostatin acts with a the same mechanism of Taxol: inhibits cancer cell growth through the stabilization of cellular microtubules
- Dictyostatin is extremely active against Taxol®-resistant tumor cell lines

Total syntheses of Dictyostatin



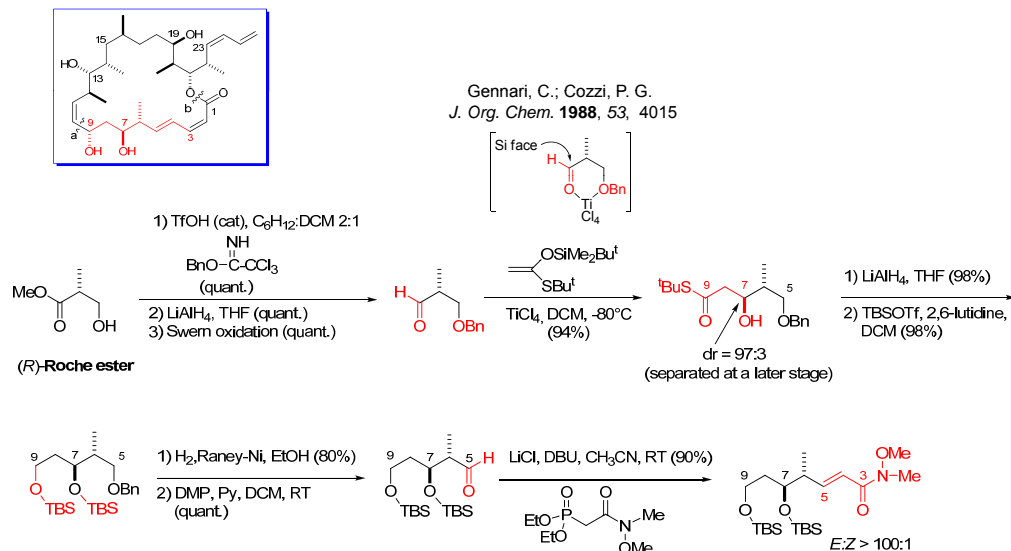
- As is often the case for natural products extracted from marine organisms, supply is insufficient for extensive *in vitro* studies, determination of Structure-Activity Relationships (SAR), *in vivo* studies, and eventually advancement to clinical trials. The need of a partially or fully synthetic approach is therefore motivated by the scarcity rather than by the beauty and fascination of their challenging molecular architecture
- Four different Total Syntheses of Dictyostatin have been described in the period 2004-2009 by Paterson, Curran, Phillips and Ramachandran

Retrosynthetic approach to Dictyostatin



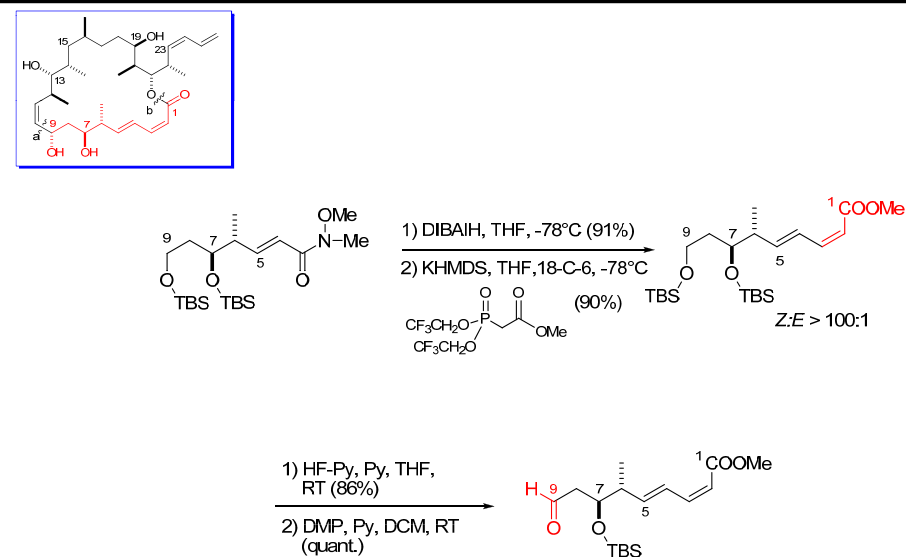
Synthesis of fragment C3-C9

Key-step: chelation controlled aldol condensation



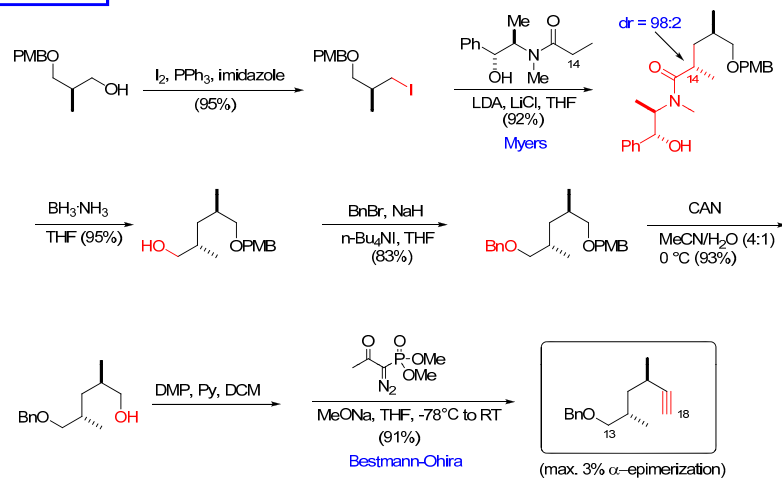
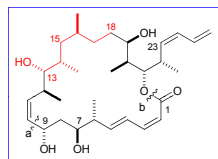
Synthesis of fragment C1-C9

Key-step: Still-Gennari olefination



Synthesis of fragment C13-C18

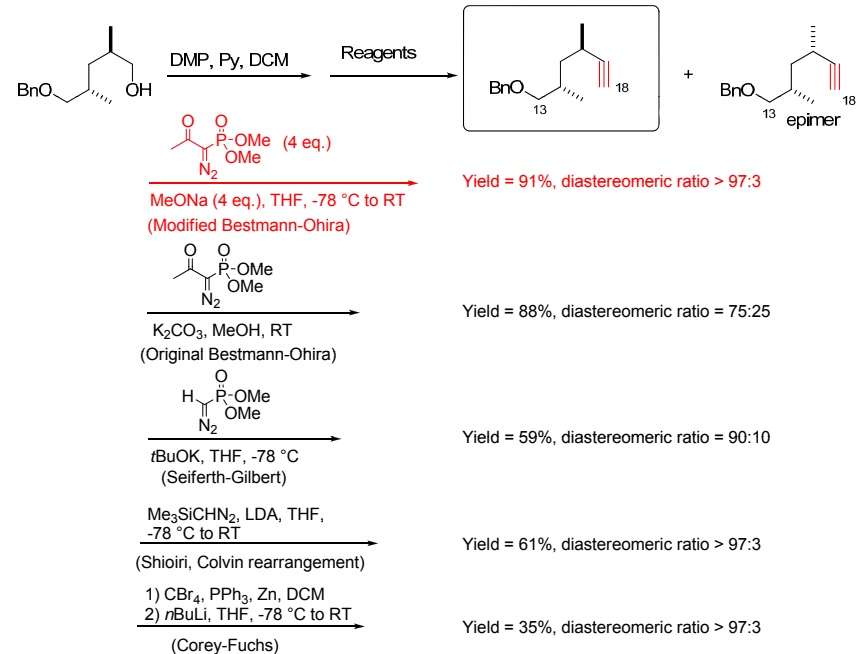
Key-steps: Myers alkylation, Bestmann-Ohira alkynylation



Monti, C.; Sharon, O.; Gennari, C. *Chem. Commun.* **2007**, 4271.

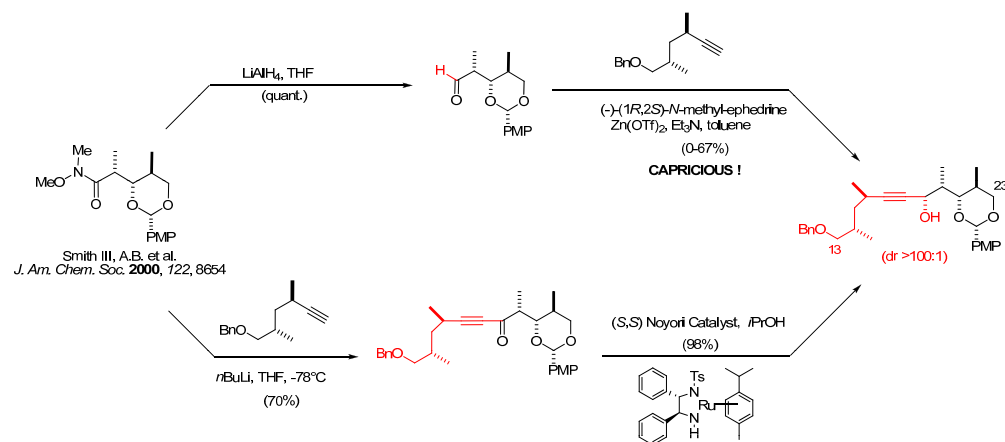
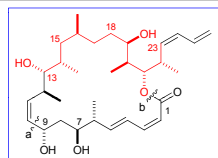
Synthesis of fragment C13-C18

Key-step: Bestmann-Ohira alkynylation

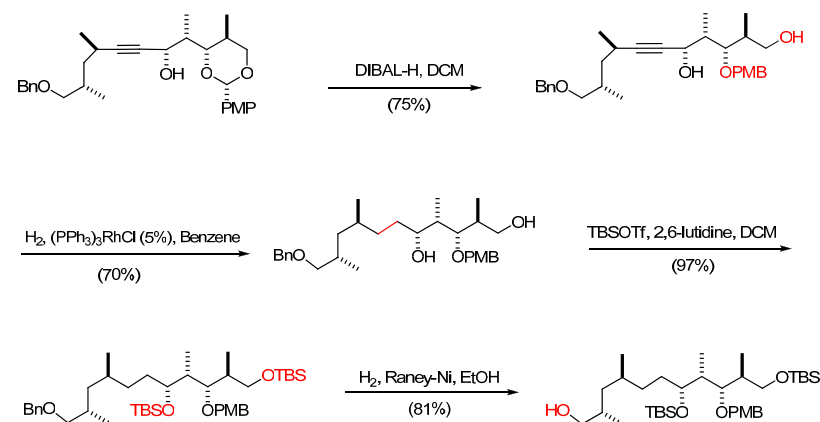
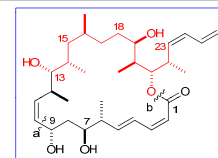


Synthesis of fragment C13-C23

Key-step: Carreira coupling vs. Noyori transfer hydrogenation

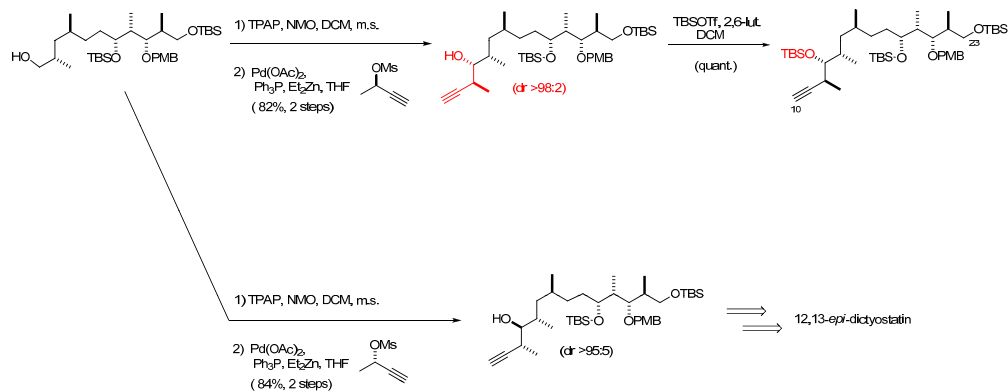
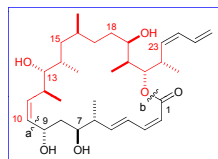


Synthesis of fragment C13-C23



Synthesis of fragment C10-C23

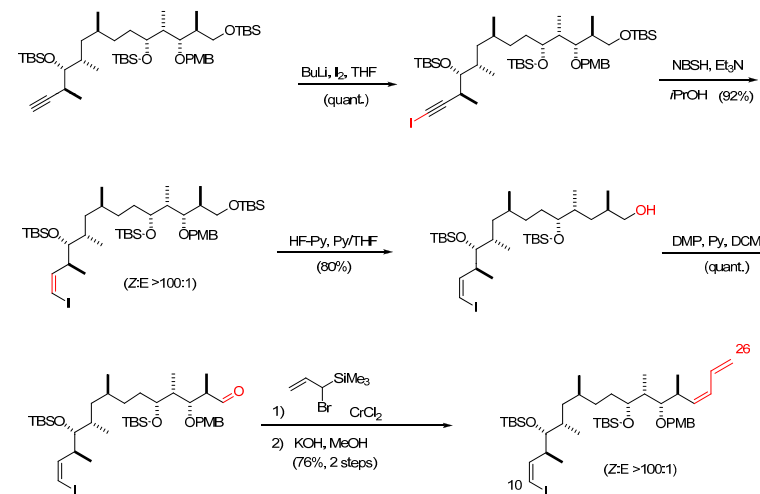
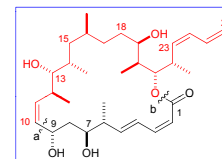
Key-step: Marshall-Tamaru allenylzinc addition



Monti, C.; Sharon, O.; Gennari, C. *Chem. Commun.* **2007**, 4271.

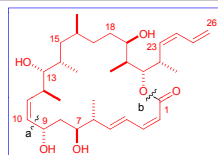
Synthesis of fragment C10-C26

Key-step: Nozaki-Hiyama-Kishi

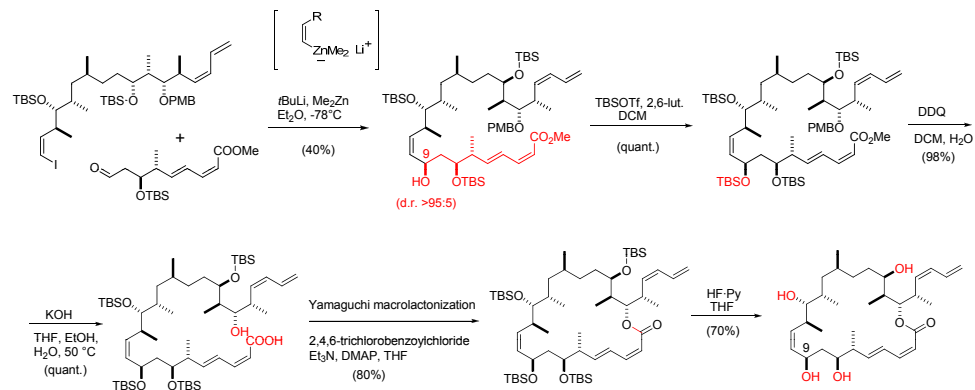


Synthesis of 9-*epi*-dictyostatin

Key-step: lithium Z-vinylzincate coupling



Ramachandran, P. V. et al. *Org. Lett.* **2007**, 9, 157



C. Zanato, L. Pignataro, A. Ambrosi, Z. Hao, C. Gennari *Eur. J. Org. Chem.* **2010**, early view.

Compared with an authentic sample kindly provided by Prof. Ian Paterson, University of Cambridge

lithium Z-vinylzincate coupling

1,3-asymmetric induction models

